Journal of Advanced Research (2016) 7, 360–372

Cairo University

Journal of Advanced Research

ORIGINAL ARTICLE

Short-term bulk energy storage system scheduling for load leveling in unit commitment: modeling, optimization, and sensitivity analysis

Reza Hemmati, Hedayat Saboori *

Department of Electrical Engineering, Kermanshah University of Technology, Kermanshah, Iran

GRAPHICAL ABSTRACT

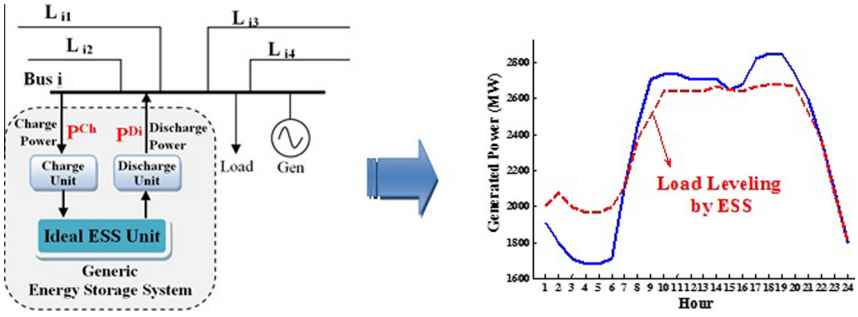

ARTICLE INFO

Article history:
Received 25 October 2015
Received in revised form 9 January 2016
Accepted 10 February 2016
Available online 18 February 2016

Keywords:
Bulk energy storage system

ABSTRACT

Energy storage systems (ESSs) have experienced a very rapid growth in recent years and are expected to be a promising tool in order to improving power system reliability and being economically efficient. The ESSs possess many potential benefits in various areas in the electric power systems. One of the main benefits of an ESS, especially a bulk unit, relies on smoothing the load pattern by decreasing on-peak and increasing off-peak loads, known as load leveling. These devices require new methods and tools in order to model and optimize their effects in the power system studies. In this respect, this paper will model bulk ESSs based on the several technical characteristics, introduce the proposed model in the thermal unit commitment (UC) problem, and analyze it with respect to the various sensitive parameters. The technical limitations of

* Corresponding author. Tel.: +98 831 7259980 2; fax: +98 831 7244201.
E-mail address: h.saboori@kut.ac.ir (H. Saboori).

Peer review under responsibility of Cairo University.

Production and hosting by Elsevier

http://dx.doi.org/10.1016/j.jare.2016.02.002

Load leveling
Mixed integer linear programming
Short-term storage scheduling
Unit commitment

the thermal units and transmission network constraints are also considered in the model. The proposed model is a Mixed Integer Linear Programming (MILP) which can be easily solved by strong commercial solvers (for instance CPLEX) and it is appropriate to be used in the practical large scale networks. The results of implementing the proposed model on a test system reveal that proper load leveling through optimum storage scheduling leads to considerable operation cost reduction with respect to the storage system characteristics.

Nomenclature

Sets

I, J	sets of network buses
M	set of piecewise linear generation cost function segments
N	set of thermal units
N_i	set of thermal units located at bus i
S	set of energy storage systems
S_i	set of energy storage systems located at bus i
T	set of time periods

Parameters

BG_n^0	initial on/off state of unit n
C_n^{CSU}	constant start-up cost of unit n at time period t
C_n^{CSD}	constant shutdown cost of unit n at time period t
C_i^{CLS}	constant cost of load shedding at bus i and time period t
$\mathrm{ES}_s^{\mathrm{Rated}}$	rated energy of energy storage system s
ES_s^0	initial stored energy in energy storage system s
k_n	constant coefficient of piecewise linear generation cost function of unit n
N_n^{GC}	number of segments of generation cost function of unit n
P_n^{RD}	ramp-down limit of unit n
P_n^{RU}	ramp-up limit of unit n
P_n^{SDR}	shutdown ramp limit of unit n
P_n^{SUR}	start-up ramp limit of unit n
P_n^{Min}	minimum generation capacity of unit n
P_n^{Max}	maximum generation capacity of unit n
$\mathrm{PD}_{i,t}$	demand at bus i and time period t
$\mathrm{PL}_{i,j}^{\mathrm{Max}}$	capacity of the line between buses i and j
$\mathrm{PS}_s^{\mathrm{Rated}}$	rated power of energy storage system s
$\mathrm{PS}_s^{\mathrm{CRU}}$	charge ramp-up limit of energy storage system s
$\mathrm{PS}_s^{\mathrm{CRD}}$	charge ramp-down limit of energy storage system s
$\mathrm{PS}_s^{\mathrm{DRU}}$	discharge ramp-up limit of energy storage system s
$\mathrm{PS}_s^{\mathrm{DRD}}$	discharge ramp-down limit of energy storage system s
R_t	required reserve at time period t
T_n^D	number of time periods unit n must be initially offline due to its minimum down-time constraint
$T_n^{D_0}$	number of time periods unit n has been offline prior to the first period of the time span
T_n^{MD}	minimum down-time of unit n
T_n^{MU}	minimum up-time of unit n
T_n^U	number of time periods unit n must be initially online due to its minimum up-time constraint
$T_n^{U_0}$	number of time periods unit n has been online prior to the first period of the time span
$\mathrm{XL}_{i,j,t}$	reactance of the line between buses i and j
α_n	constant coefficient of quadratic generation cost function of unit n
β_n	first order coefficient of quadratic generation cost function of unit n
γ_n	second order coefficient of quadratic generation cost function of unit n
η_s^{Ch}	charge efficiency of energy storage system s
η_s^{Di}	discharge efficiency of energy storage system s
$\lambda_{n,m}$	slope of segment m of piecewise linear generation cost function of unit n

Variables

$\mathrm{BG}_{n,t}^{\mathrm{State}}$	binary variable indicating on/off state of generating unit n at time period t
$\mathrm{BG}_{n,t}^{\mathrm{SU}}$	binary variable indicating start-up state of generating unit n at time period t
$\mathrm{BG}_{n,t}^{\mathrm{SD}}$	binary variable indicating shutdown state of generating unit n at time period t
$\mathrm{BS}_{s,t}^{\mathrm{Ch}}$	binary variable indicating charge state of energy storage system s at time period t
$\mathrm{BS}_{s,t}^{\mathrm{Di}}$	binary variable indicating discharge state of energy storage system s at time period t
$C_{i,t}^{\mathrm{LS}}$	load shedding cost at bus i and time period t
$C_{n,t}^{\mathrm{SD}}$	shutdown cost of unit n at time period t
$C_{n,t}^{\mathrm{PG}}$	generation cost of unit n at time period t
$C_{n,t}^{\mathrm{SU}}$	start-up cost of unit n at time period t
$\mathrm{ES}_{s,t}$	stored energy in energy storage system s at time period t
$P_{m,n,t}^{\mathrm{PL}}$	generated power in segment m of piecewise linear generation cost function of unit n at time period t
$P_{i,t}^{\mathrm{LS}}$	load shedding at bus i and time period t
P_t^{Res}	total reserve of the system at time period t
$\mathrm{PG}_{n,t}$	generated power of unit n at time period t
$\mathrm{PG}_{i,t}^{\mathrm{Bus}}$	sum of the generated power of units located at bus i at time period t
$\mathrm{PG}_{n,t}^{\mathrm{Max}}$	maximum producible power of unit n at time period t
$\mathrm{PG}_{n,t}^{\mathrm{Res}}$	spinning reserve of unit n at time period t
$\mathrm{PI}_{i,t}$	power injected at bus i and time period t
$\mathrm{PL}_{i,j,t}$	flow of the line between buses i and j at time period t

$PS^{Ch}_{s,t}$	charged power into energy storage system s at time period t	$T^{D}_{n,t}$	number of time periods unit n has been offline prior to the start-up in time period t
$PS^{Di}_{s,t}$	discharged power from energy storage system s at time period t	$\delta_{i,t}$	voltage angle of bus i at time period t

Introduction

An energy storage system (ESS) is defined as a device with capability of storing electric energy in charging periods and delivering stored energy at discharging periods, when needed [1]. Different from other apparatus utilized in the electric power system, ESSs have a variety of technologies and functionalities. These devices can act as a controllable load or an adjustable generator giving them the ability to offer many diverse applications, regarding the installation location, their characteristics, and control procedure [2]. The ESSs installed within an electricity system can be provided by a range of technologies [3]. The ESS technologies include hydraulic pumped energy storage (HPES), compressed air energy storage (CAES), flywheel energy storage (FWES), superconducting magnetic energy storage (SMES), battery energy storage system (BESS), and supercapacitor or ultracapacitor energy storage (SCES). The ESS technologies can be broadly categorized into two groups, including centralized bulk power storage and distributed storage. The centralized bulk energy storage technologies, also known as large-scale or grid-scale storage, are relatively large installations designed to store large amounts of electricity where storage capacity ranges from tens to hundreds of megawatts, and the units can supply power to the grid for hours at a time [4]. The HPES, CAES, and advanced large-scale batteries belong to this category. Distributed multipurpose power storage technologies include dispersed ESSs in the power system and are used either to meet specific and local applications (customer power quality issues, microgrid islanding, costumer peak shaving, and et cetera) or grid scale services to the system operator (including voltage support, frequency regulation, load shifting, and so on). These technologies can be located at generating plants, on the power transmission or distribution systems, or at an end-user site including FWES, SMES, SCES, and small-scale and medium-scale battery energy storage technologies [5]. The ESSs have experienced a very rapid growth in recent years and are expected to be a promising tool in order to improving power system reliability and economics [6,7]. With this outlook, bulk storage devices are expected to be incorporated into power systems in the near future [8,9]. The ESSs possess many potential benefits in various areas in the electric power systems [10]. As a consequence, these devices are increasing their impact on the utility grid as a solution to the existing problems. The potential applications of the EESs in the electric power systems including power quality improvement, ride-through capability (bridging power), energy management, integrating and smoothing intermittent renewable resources, emergency back-up power, telecommunications back-up, ramping and load following, peak shaving, time shifting, load leveling, seasonal energy storage, low voltage ride-through, transmission and distribution stability, black-start, voltage regulation and control, network fluctuation suppression, spinning reserve, end-user electricity service reliability, motor starting, uninterruptible power supply, and transmission and distribution upgrade deferral have been widely reported in recent years and are out of the scope of this work [2,6,9,10]. But, the main reported applications of the ESSs are load leveling, renewable resources integration and smoothing, frequency regulation and stabilization, and transmission and distribution network upgrade [2,11]. It should be noted that each application requires specific storage characteristics in terms of power and energy rating and charge and discharge duration. Each of these major applications is reviewed in the following, briefly.

Load leveling (energy time shift)

Load leveling refers to the smoothing of the load pattern by lowering on-peak and increasing off-peak loads. The load leveling is also defined as charging ESS by purchased cheap electric energy at periods when prices are low and discharge ESS to sell stored energy at a later time when the prices are high. In principle, energy time-shift includes potential energy transactions with financial advantage based on the differences between the cost to purchase energy (charge) and sell it (discharge). In addition to cost saving, load leveling reduces the need to utilize peaking power plants or augment the transmission and distribution infrastructure. Functional candidates for peak shaving application are pumped hydro energy storage, compressed air energy storage, and large-scale batteries. Related studies of this application were previously reported [12–19].

Renewable integration and smoothing

Nowadays, renewable energy resources are penetrated into the electric power systems as large scale plants. The statistics indicate that wind and solar energy projects are the fastest-growing renewable energy resources in the world, due to their sustainability, cleanness, and cost effectiveness compared to the other renewable energy resources [20,21]. The uncertainty is the main problem to utilize these resources because the wind speed and solar radiation are continuously changing and afterward, the output power of the plant will be changed. These power fluctuations can cause considerable troubles in terms of voltage and frequency stability. In the electric power systems equipped with these renewable resources, a suitable mechanism should be utilized in order to overcome power fluctuations. In this regard, it is demonstrated that energy storage systems will have a vital role to accommodate renewable resources in both connected and isolated plants. The inherent intermittent renewable generation can be suppressed, steadied or smoothed by means of integration with storage units [22–28].

Frequency regulation and stabilization

Frequency stability refers to the capability of a power system to preserve steady frequency following a serious disturbance leading to a considerable imbalance between generation and

load. It relies on the ability to bring back equilibrium between system generation and load, with smallest load shedding [29]. In order to regulate the system frequency dynamically during the transients caused by disturbances or sudden changes, storage units can utilize to maintain frequency stability [30,31]. In this context, batteries [32–35], superconducting magnetic energy storage (SMES) systems [36–39], supercapacitors [40–42], and flywheels [43,44] are well-suited for this application.

Transmission and distribution network upgrade

Energy storage systems can be employed in order to upgrade the operation and planning of the transmission and distribution network [45]. For instance, they can reduce congestion [46–48] and defer investment in transmission network [49–51] and also reduce losses [52], improve reliability [53], and defer investment decision [54] in distribution network. Relatively large power capacity compared with system demand is important for such applications.

As discussed above, various applications are defined for the ESSs in the literature and are quantified and analyzed with exact case studies [11–54]. In this paper, application of a bulk ESS unit to level load profile is quantified in detail in a thermal unit commitment context (UC). The proposed model is a Mixed Integer Linear Programming (MILP) which can be easily solved by strong commercial solvers (for instance CPLEX as used in this paper) and it is appropriate to be used in the practical large scale networks. The ESSs are modeled with respect to the various technical characteristics and their role to level load profile is analyzed regarding governing factors. The proposed model is tested on IEEE 24 bus reliability test system (RTS) and is solved using GAMS software. Additionally, optimal charge/discharge schedule of the ESSs in order to achieve minimum operation cost is obtained while considering thermal units and transmission network constraints.

The remaining sections of the paper are organized as follows. Section 'Proposed formulation' introduces main network constrained MILP unit commitment model without storage devices, and provides a detailed description and modeling of the energy storage system. Afterward, complete proposed UC model incorporating new equations representing storage devices is given in the end of this section. Results of implementing the proposed model on the test system are presented and discussed in the Section 'Case study'. Finally, in Section 'Conclusions', some relevant conclusions are given.

Proposed formulation

In this section, the main unit commitment problem without ESS is formulated firstly. Then, the ESS is modeled with respect to the various technical characteristics. Finally, the complete proposed model for the ESS integration and scheduling in the thermal unit commitment is presented.

MILP unit commitment without storage device

Unit Commitment (UC) is defined as to turn a generating unit on, which includes speeding up the unit, synchronizing and connecting it to the grid so it is able to deliver the power [55]. Regarding the power demand variations, the UC problem is to commit adequate units at appropriate time and with enough generated power, economically. In addition, most of the unit types in the electric power systems are the thermal units which cannot instantly turn on and produce power. Therefore, the UC problem must be solved in advance so that enough producible power is always accessible to supply the system demand [56]. A variety of methods have been proposed to model and solve the UC problem [57], but mixed integer linear programming (MILP) is a well-known method providing various advantages over other ones. The MILP convergence to the optimal solution is guaranteed in a finite number of the iterations while a flexible and accurate modeling framework is provided. Furthermore, during search of the problem space, information on the proximity to the optimal solution is available [58–62]. Professional MILP softwares based on the branch and bound, and branch and cut algorithms have been widely developed and commercial packages with large-scale capabilities are currently available and used extensively [63,64].

The main unit commitment formulation without storage devices described in this subsection is based on the model presented by Carrio and Arroyo [59]. The power generation, start-up, and shutdown costs, and also the technical constraints of the thermal units are considered in the problem formulation. Transmission network constraints and cost of the load shedding are also added to the model. The constituents of the proposed formulation including objective function and its cost components, power balance equations, reserve requirements, and thermal constraints have been described in the following, respectively.

The objective function of the unit commitment problem is considered as follows:

$$\text{Min} \sum_{t\in T}\sum_{n\in N}\sum_{i\in I}\left(C^{\text{PG}}_{n,t}+C^{\text{SU}}_{n,t}+C^{\text{SD}}_{n,t}+C^{\text{LS}}_{i,t}\right) \tag{1}$$

The objective function presented in (1) is equal to the daily total operation cost of the system. As the equation denotes, total operation cost is equal to four terms including power generation, start-up, and shutdown costs of the units in addition to the cost of the load shedding. In this equation, variable C with subscripts n and t denotes a cost term related to unit n and at time period t. Also, superscripts PG, SU, and SD stand for power generation, start-up, and shutdown, respectively. The latest cost component, cost of load shedding are presented by $C^{\text{LS}}_{i,t}$ where superscript LS and subscripts i and t stand for load shedding, bus I, and time period t, respectively.

Generation cost function of the thermal units is usually defined as a quadratic function of the output power as formulated in (2). In this equation, $\text{PG}_{n,t}$ refers to the generated power by unit n at time period t while binary variable $\text{BG}^{\text{State}}_{n,t}$ is equal to 1 if unit n at time period t is online and equal to 0 otherwise. Parameters α_n, β_n, and γ_n indicate constant, first order, and second order cost coefficients, respectively.

$$C^{\text{PG}}_{n,t}=\alpha_n\times\text{BG}^{\text{State}}_{n,t}+\beta_n\times\text{PG}_{n,t}+\gamma_n\times\text{PG}^2_{n,t}\qquad\forall\, n\in N,\ \forall\, t\in T \tag{2}$$

Therefore, the resulting objective function is a non-linear function. In order to guarantee convergence of the optimal solution, a linear approximation should be applied to the cost function. The nonlinear (quadratic) cost function curve is shown in Fig. 1. As shown in Fig. 1, the non-linear cost function can be accurately approximated with a sequence of straight line segments. In the figure, the variables $P_{1,n}$, $P_{2,n}$ and $P_{3,n}$ denote generation increments and range from 0 to

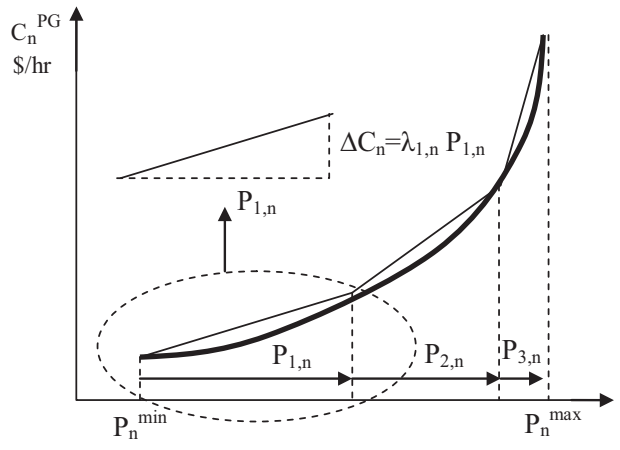

Fig. 1 Piecewise linear approximation of the quadratic cost function curve.

respective maximum values. It should be noted that $P_{m,n}$ is not the generation value by itself. In other word, sum of the minimum power output and generation segments will be equal to the total generated power. If $\lambda_{m,n}$ represents the slope of the line segment m, then the increment in cost function corresponding to this line segment is equal to $\lambda_{m,n}\ P_{m,n}$. The fitness of this so-called "piecewise linear" approximation method can be improved to any preferred level by increasing the number of used line segments. By adding subscript t standing for time period, Eqs. (3)–(5) formulate this approximation.

$$k_n = \alpha_n + \beta_n \times \mathrm{PG}_n^{\mathrm{Min}} + \gamma_n \times \left(\mathrm{PG}_n^{\mathrm{Min}}\right)^2 \qquad \forall\ n \in N \tag{3}$$

$$C_{n,t}^{\mathrm{PG}} = k_n \times \mathrm{BG}_{n,t}^{\mathrm{State}} + \sum_{m=1}^{N_n^{\mathrm{GC}}} \left(\lambda_{m,n} \times P_{m,n,t}^{\mathrm{PL}}\right) \qquad \forall\ n \in N, \quad \forall\ t \in T \tag{4}$$

$$\mathrm{PG}_{n,t} = PG_n^{\mathrm{Min}} \times \mathrm{BG}_{n,t}^{\mathrm{State}} + \sum_{m=1}^{N_n^{\mathrm{GC}}} P_{m,n,t}^{\mathrm{PL}} \qquad \forall\ n \in N, \quad \forall\ t \in T \tag{5}$$

In (3), parameter k_n, is equal to the cost of the generated power corresponding to the minimum power output point. As the equation denotes, this parameter is calculated through replacing $\mathrm{PG}_{n,t}$ by $\mathrm{PG}_n^{\mathrm{Min}}$ in (2). Eq. (4) shows that if unit n is online, then cost of the generated power will be equal to the sum of the cost of the power generation segments in addition to cost of the minimum power output of the unit (i.e. k_n). Finally, Eq. (5) states that total generated power is equal to sum of the power generation segments in addition to the minimum power output of the unit.

The start-up cost of the units is calculated by (6)–(8) where binary variable $\mathrm{BG}_{n,t}^{\mathrm{SU}}$ represents start-up situation of each unit at each time period. This binary variable is equal to 1 if unit n at time period t is started-up and 0 otherwise. In other words, this binary variable at each time period is equal to on/off status of the unit at present time period minus its situation at previous time period (see (6)). In (7), start-up cost for each unit at each time period is calculated via multiplying corresponding start-up binary variable by unit constant start-up cost denoted by C_n^{CSU}. Regarding positive value of the constant start-up cost $\left(C_n^{CSU}\right)$ and free value of the start-up binary variable $\left(\mathrm{BG}_{n,t}^{\mathrm{SU}}\right)$ which may be a positive or negative value, resulting start-up cost can be either positive or negative. Only positive start-up values are acceptable, as declared in (8).

$$\mathrm{BG}_{n,t}^{\mathrm{SU}} = \left[\mathrm{BG}_{n,t}^{\mathrm{State}} - BG_{n,t-1}^{\mathrm{State}}\right] \qquad \forall\ n \in N, \quad \forall\ t \in T \tag{6}$$

$$C_{n,t}^{\mathrm{SU}} = C_n^{CSU}\mathrm{BG}_{n,t}^{\mathrm{SU}} \qquad \forall\ n \in N, \quad \forall\ t \in T \tag{7}$$

$$C_{n,t}^{\mathrm{SU}} \geqslant 0 \qquad \forall\ n \in N, \quad \forall\ t \in T \tag{8}$$

Like the start-up cost, shutdown cost can be simply calculated as (9)–(11). In these equations, binary variable $\mathrm{BG}_{n,t}^{\mathrm{SD}}$ stands for shutdown status of unit n at time period t while parameter C_n^{CSU} represents constant shutdown cost of unit n.

$$\mathrm{BG}_{n,t}^{\mathrm{SD}} = \left[\mathrm{BG}_{n,t-1}^{\mathrm{State}} - BG_{n,t}^{\mathrm{State}}\right] \qquad \forall\ n \in N, \quad \forall\ t \in T \tag{9}$$

$$C_{n,t}^{\mathrm{SD}} = C_n^{\mathrm{CSD}}\mathrm{BG}_{n,t}^{\mathrm{SD}} \qquad \forall\ n \in N, \quad \forall\ t \in T \tag{10}$$

$$C_{n,t}^{\mathrm{SD}} \geqslant 0 \qquad \forall\ n \in N, \quad \forall\ t \in T \tag{11}$$

Cost of the load shedding is equal to the value of the shed load multiplied by amount of the shed load as denoted by (12). In this equation, parameter C_i^{CLS} and variable $P_{i,t}^{\mathrm{LS}}$ denote constant load shedding cost at bus i and amount of the shed load at bus i and time period t. The amount of shed load should be a positive value and smaller than the bus power demand to ensure that fictitious power is not generated. Eqs. (13) and (14) guarantee this situation where $\mathrm{PD}_{\mathrm{i,t}}$ refers to power demand of bus i at time period t.

$$C_{i,t}^{\mathrm{LS}} = C_i^{\mathrm{CLS}} P_{i,t}^{\mathrm{LS}} \qquad \forall\ i \in I, \quad \forall\ t \in T \tag{12}$$

$$P_{i,t}^{\mathrm{LS}} \leqslant \mathrm{PD}_{i,t} \tag{13}$$

$$P_{i,t}^{\mathrm{LS}} \geqslant 0 \qquad \forall\ i \in I, \quad \forall\ t \in T \tag{14}$$

Constraint (15) is used to balance the power generation and consumption in the real-time in every bus of the system. According to this constraint, sum of the generated power of the thermal units plus load shedding in each bus should be equal to the power demand plus injected power to the lines connected to the bus. In this equation, $\mathrm{PG}_{i,t}^{\mathrm{Bus}}$, $P_{i,t}^{\mathrm{LS}}$, $\mathrm{PD}_{i,t}$, and $\mathrm{PI}_{i,t}$ respectively denote total generated power, load shedding, power demand, and total injected power at bus i and time period t. Eq. (16) states that overall generated power at each bus is equal to the sum of the generated power of the units installed in the bus. Eq. (17) calculates power injected into the bus as a function of flow of the lines connected to the bus ($\mathrm{PL}_{i,j,t}$).

$$\mathrm{PG}_{i,t}^{\mathrm{Bus}} + P_{i,t}^{\mathrm{LS}} = \mathrm{PD}_{i,t} + \mathrm{PI}_{i,t} \qquad \forall\ i \in I, \quad \forall\ t \in T \tag{15}$$

$$\mathrm{PG}_{i,t} = \sum_{n \in N_i} \mathrm{PG}_{n,t} \qquad \forall\ i \in I, \quad \forall\ t \in T \tag{16}$$

$$\mathrm{PI}_{i,t} = \sum_{j \in J} \mathrm{PL}_{i,j,t} \qquad \forall\ i,\ j \in I, \quad \forall\ t \in T \tag{17}$$

Flow of the lines is calculated based on the DC power flow equation. The linear, non-complex, and non-iterative characteristic of the DC power flow attracts considerable analytical

and computational attention. In contrast to the AC power flow model, the advantages of a DC model are as follows [65]:

- Its solution method is non-iterative as well as the results are reliable and unique.
- The problems can be modeled, solved, and optimized efficiently by using its method.
- Required network data are minimum and comparatively easy to obtain.

On the other hand, sometimes there may be no practical alternative to the use of the DC power flow. For instance and as in our case, using DC power flow is inevitable when computational burden of the problem is high due to the use of binary variables or modeling large scale practical transmission networks. In addition, only way to keep linearity of the model in the transmission constraint problems is to use this approximation [66]. In DC power flow model, by ignoring transmission line losses, the magnitude of the active power injected into (P_{ij}) and drawn from (P_{ji}) the line will be equal to

$$\mathrm{PL}_{i,j} = -PL_{j,i} = PL_{i,j} = \frac{V_i V_j \mathrm{Sin}(\delta_i - \delta_j)}{\mathrm{XL}_{i,j}} \tag{18}$$

where XL_{ij} denotes the line reactance and V and δ represent voltage magnitude and angle at sending and receiving buses to which the line is connected. Then, it is assumed that in normal operation conditions, bus voltage magnitudes are almost equal to 1 per-unit (see Eq. (19)) and bus voltage angles are small enough to assume that their sinus is equal to themselves in radians as declared in (20).

$$V_1 \approx V_2 \approx 1 \tag{19}$$

$$\mathrm{Sin}(\delta_1 - \delta_2) \gg \delta_1 - \delta_2 \tag{20}$$

Substituting (19) and (20) in (18), we have

$$\mathrm{PL}_{i,j} = \frac{\delta_i - \delta_j}{\mathrm{XL}_{i,j}} \tag{21}$$

By adding subscript t denoting time period, DC line flow equation will be

$$\mathrm{PL}_{i,j,t} = \frac{\delta_{i,t} - \delta_{j,t}}{\mathrm{XL}_{i,j}} \qquad \forall\ i,\ j \in I, \quad \forall\ t \in T \tag{22}$$

Finally, Eq. (23) enforces line flow limits in both directions where parameter $\mathrm{PL}_{i,j}^{\mathrm{Max}}$ represents maximum allowable line flow.

$$-PL_{i,j}^{\mathrm{Max}} \leqslant \mathrm{PL}_{i,j,t} \leqslant \mathrm{PL}_{i,j}^{\mathrm{Max}} \qquad \forall\ i,\ j \in I, \quad \forall\ t \in T \tag{23}$$

As it is shown in (24), spinning reserve of an online unit (denoted by variable $\mathrm{PG}_{n,t}^{\mathrm{Res}}$) is equal to its maximum producible power (denoted by parameter $\mathrm{PG}_{n,t}^{\mathrm{Max}}$) minus its generated power. The summation over spinning reserves of all units yields system spinning reserve, or P_t^{Res}, as stated in (25). This value at each time period should be greater than the minimum required reserve of the system (denoted by parameter R_t) as declared in (26).

$$\mathrm{PG}_{n,t}^{\mathrm{Res}} = \mathrm{PG}_{n,t}^{\mathrm{Max}} - PG_{n,t} \qquad \forall\ n \in N, \quad \forall\ t \in T \tag{24}$$

$$P_t^{\mathrm{Res}} = \sum_{n \in N} \mathrm{PG}_{n,t}^{\mathrm{Res}} \qquad \forall\ t \in T \tag{25}$$

$$P_t^{\mathrm{Res}} \geqslant R_t \qquad \forall\ t \in T \tag{26}$$

The constraints including the technical constraints of the thermal units such as generation limits, ramp-up, ramp-down, start-up ramp, shutdown ramp, minimum up-time, and minimum down time are declared in (27)–(39). These equations are a reformulation of the model presented before [61] and any other similar model (i.e. MILP UC models) can be replaced simply because of independency of them with respect to rest of the model. Detailed description of each equation was previously provided [59] and out of scope of this paper.

$$P_n^{\mathrm{Min}} \mathrm{BG}_{n,t}^{\mathrm{State}} \leqslant \mathrm{PG}_{n,t} \leqslant \mathrm{PG}_n^{\mathrm{Max}} \qquad \forall\ n \in N, \quad \forall\ t \in T \tag{27}$$

$$0 \leqslant \mathrm{PG}_{n,t}^{\mathrm{Max}} \leqslant P_n^{\mathrm{Max}} \mathrm{BG}_{n,t}^{\mathrm{State}} \qquad \forall\ n \in N, \quad \forall\ t \in T \tag{28}$$

$$\mathrm{PG}_{n,t}^{\mathrm{Max}} \leqslant \mathrm{PG}_{n,t-1} + P_n^{\mathrm{RU}} \mathrm{BG}_{n,t-1}^{\mathrm{State}} + P_n^{\mathrm{SUR}} \times \mathrm{BG}_{n,t}^{\mathrm{SU}} + P_n^{\mathrm{Max}} \left(1 - BG_{n,t}^{\mathrm{State}}\right) \qquad \forall\ n \in N, \quad \forall\ t \in T \tag{29}$$

$$\mathrm{PG}_{n,t-1}^{\mathrm{Max}} \leqslant P_n^{\mathrm{Max}} \mathrm{BG}_{n,t}^{\mathrm{State}} + P_n^{\mathrm{SD}} \mathrm{BG}_{n,t}^{\mathrm{SD}} \qquad \forall\ n \in N, \quad \forall\ t \in T \tag{30}$$

$$\mathrm{PG}_{n,t-1} \leqslant \mathrm{PG}_{n,t} + P_n^{\mathrm{RD}} \mathrm{BG}_{n,t}^{\mathrm{State}} + P_n^{\mathrm{SDR}} \times \mathrm{BG}_{n,t}^{\mathrm{SD}} + \mathrm{PG}_n^{\mathrm{Max}} \left(1 - BG_{n,t-1}^{\mathrm{State}}\right) \qquad \forall\ n \in N, \quad \forall\ t \in T \tag{31}$$

$$T_n^U = \min\left\{T, \left[T_n^{\mathrm{MU}} - T_n^{U_0}\right] \times \mathrm{BG}_n^0\right\} \qquad \forall\ n \in N \tag{32}$$

$$\sum_{t=1}^{T_n^U} \left(1 - \mathrm{BG}_{n,t}^{\mathrm{State}}\right) = 0 \qquad \forall\ n \in N \tag{33}$$

$$\sum_{i=t}^{t+T_n^{\mathrm{MU}}-1} \mathrm{BG}_{n,i}^{\mathrm{State}} \geqslant T_n^{\mathrm{MU}} \times \mathrm{BG}_{n,t}^{\mathrm{SU}} \qquad \forall\ n \in N, \quad \forall\ t = T_n^U + 1, \ldots, T - T_n^{\mathrm{MU}} + 1 \tag{34}$$

$$\sum_{i=t}^{T} \left[\mathrm{BG}_{n,t}^{\mathrm{State}} - \mathrm{BG}_{n,t}^{\mathrm{SU}}\right] \geqslant 0 \qquad \forall\ n \in N, \quad \forall\ t = T - T_n^{\mathrm{MU}} + 2, \ldots, T \tag{35}$$

$$T_n^D = \min\left\{T, \left[T_n^{\mathrm{MD}} - T_n^{D_0}\right] \times \left(1 - BG_n^0\right)\right\} \tag{36}$$

$$\sum_{t=1}^{T_n^D} \mathrm{BG}_{n,i}^{\mathrm{State}} = 0 \qquad \forall\ n \in N \tag{37}$$

$$\sum_{i=t}^{t+T_n^{\mathrm{MD}}-1} \left(1 - \mathrm{BG}_{n,i}^{\mathrm{State}}\right) \geqslant T_n^{\mathrm{MD}} \times \mathrm{BG}_{n,t}^{\mathrm{SD}} \qquad \forall\ n \in N, \quad \forall\ t = T_n^D + 1, \ldots, T - T_n^{\mathrm{MD}} + 1 \tag{38}$$

$$\sum_{i=t}^{T} \left[1 - \mathrm{BG}_{n,i}^{\mathrm{State}} - \mathrm{BG}_{n,i}^{\mathrm{SD}}\right] \geqslant 0 \qquad \forall\ n \in N, \quad \forall\ t = T - T_n^{\mathrm{MD}} + 2, \ldots, T \tag{39}$$

Proposed energy storage system model

Energy storage systems (ESSs) installed within an electricity system can be provided by a range of technologies [2,3,5,6]. As discussed in the introduction, the ESS technologies can be broadly categorized into two groups, including centralized bulk power storage and distributed storage [67]. Irrespective of the ESS technology type, an ESS can be modeled approximately by an ideal ESS unit along with its charge/discharge units, as depicted in Fig. 2. This assumption is completely acceptable for the purposes of this paper.

As the figure shows, some of the charged power into and discharged power from the ESS will lose in the conversion devices. The percent of the charge efficiency enforced by charging unit determines the relation between power drawn from the grid and net power charged into the ESS. In other words, if P^{Ch} and η_C denote charge power drawn from the bus and charging unit efficiency, then net power charged into the ESS (excluding charging losses) will be equal to $P^{\mathrm{Ch}}\ \eta_C$. Like the charge state, discharge state is affected from discharging unit. It should be noted that, discharged power drawn from the ESS is equal to the net discharging power injected into the grid at ESS installation bus (without discharge losses) in addition to the discharging unit losses. In other words, if P^{Di} and η_{Di} denote net discharge power injected into the bus and discharging unit efficiency, then power discharged from the ESS (including discharging losses) will be equal to $P^{\mathrm{Di}}/\eta_{\mathrm{Di}}$. This matter should be regarded in the power balance and ESS energy balance equations in bus at which the ESS is installed. Eq. (40) simplifies the above matter and modifies the power balance equation presented in (15) in order to account for the ESS installation in the bus. As the equation shows, an ESS unit can be modeled as a controllable load and a generating unit to represent charge and discharge states, respectively. In this equation, variables $\mathrm{PS}^{\mathrm{Ch}}_{s,t}$ and $\mathrm{PS}^{\mathrm{Di}}_{s,t}$ are respectively charging power drawn from and discharging power injected into the bus by energy storage s at time period t while other variables are as (15). It should be noted that all of the charging powers to and discharging powers from installed ESS units in bus i (denoted by set S_i) should be summed up as declared by (40).

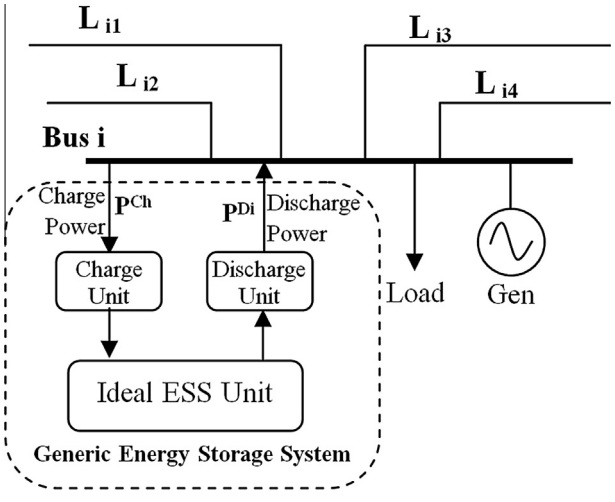

Fig. 2 Modeling of a generic energy storage system.

$$\mathrm{PG}^{\mathrm{Bus}}_{i,t} + P^{\mathrm{LS}}_{i,t} + \sum_{s\in S_i}\mathrm{PS}^{\mathrm{Di}}_{s,t} = \mathrm{PD}_{i,t} + \mathrm{PI}_{i,t} + \sum_{s\in S_i}\mathrm{PS}^{\mathrm{Ch}}_{s,t} \qquad \forall\ i \in I,\ \forall\ s \in S \tag{40}$$

Eqs. (41) and (42) enforce that stored energy in the ESS in the beginning ($t = 1$) and the end of the time period ($t = T$) must be equal to the initial stored energy because of the periodical nature of the problem. In these equations, parameter ES^0_s denotes initial stored energy in energy storage s and variable $\mathrm{ES}_{s,t}$ stands for stored energy in the energy storage s at time period t.

$$\mathrm{ES}_{s,t} = \mathrm{ES}^0_s \qquad \forall\ t = 1 \tag{41}$$

$$\mathrm{ES}_{s,t} = \mathrm{ES}^0_s \qquad \forall\ t = T \tag{42}$$

Energy balance equation of the ESS is declared in (43). This equation means that stored energy at each time period is equal to the stored energy at the previous time period plus net charged power into and minus gross discharged power from the ESS at present time period. Also, the stored energy in the ESS is a positive value (see (44)) limited to its energy rating as stated in (45).

$$\mathrm{ES}_{s,t} = \mathrm{ES}_{s,t-1} + \mathrm{PS}^{\mathrm{Ch}}_{s,t}\eta_{\mathrm{Ch}} - \mathrm{PS}^{\mathrm{Di}}_{s,t}/\eta_{\mathrm{Di}} \qquad \forall\ t \in T,\quad \forall\ s \in S \tag{43}$$

$$\mathrm{ES}_{s,t} \leqslant \mathrm{ES}^{\mathrm{Rated}}_s \qquad \forall\ t \in T,\quad \forall\ s \in S \tag{44}$$

$$\mathrm{ES}_{s,t} \geqslant 0 \qquad \forall\ t \in T,\quad \forall\ s \in S \tag{45}$$

The ESS at every time period may be in one of the charge or discharge states or in the idle state. In other words, charge and discharge states cannot take place simultaneously at a single time period. This situation is modeled by adding two binary variables indicating charge state denoted by $\mathrm{BS}^{\mathrm{Ch}}_{s,t}$ and discharge state denoted by $\mathrm{BS}^{\mathrm{Di}}_{s,t}$. As Eq. (46) confirmed, the ESS among actions charge, discharge, and doing nothing must be chose one and cannot perform joint actions at each time period.

$$\mathrm{BS}^{\mathrm{Ch}}_{s,t} + \mathrm{BS}^{\mathrm{Di}}_{s,t} \leqslant 1 \qquad \forall\ t \in T,\quad \forall\ s \in S \tag{46}$$

Charge and discharge units of the ESS restrict its maximum transferable power. Eqs. (47) and (48) confirm this restriction for charge and discharge states, respectively, provided that respective binary variables must be switched on. In these equations, $\mathrm{PS}^{\mathrm{Rated}}_s$ represents rated power of the ESS. Irrespective of discharge power rating constraint, the ESS at each time period can deliver at last all of the stored energy at previous time period multiplied by its discharge efficiency, as stated in (49).

$$\mathrm{PS}^{\mathrm{Ch}}_{s,t} \leqslant \mathrm{PS}^{\mathrm{Rated}}_s \mathrm{BS}^{\mathrm{Ch}}_{s,t} \qquad \forall\ t \in T,\quad \forall\ s \in S \tag{47}$$

$$\mathrm{PS}^{\mathrm{Di}}_{s,t} \leqslant \mathrm{PS}^{\mathrm{Rated}}_s \mathrm{BS}^{\mathrm{Di}}_{s,t} \qquad \forall\ t \in T,\quad \forall\ s \in S \tag{48}$$

$$\mathrm{PS}^{\mathrm{Di}}_{s,t} \leqslant \mathrm{ES}_{s,t-1}\eta_{\mathrm{Di}}\mathrm{BS}^{\mathrm{Di}}_{s,t} \qquad \forall\ t \in T,\quad \forall\ s \in S \tag{49}$$

Because of the technical constraints, the ESS in the charge and discharge states cannot experience power variations above allowable boundaries between the adjacent time periods. These boundaries are stated in Eqs. (50)–(53) and related to charge ramp-up, charge ramp-down, discharge ramp-up, and discharge ramp-down powers of the ESS, respectively. In these

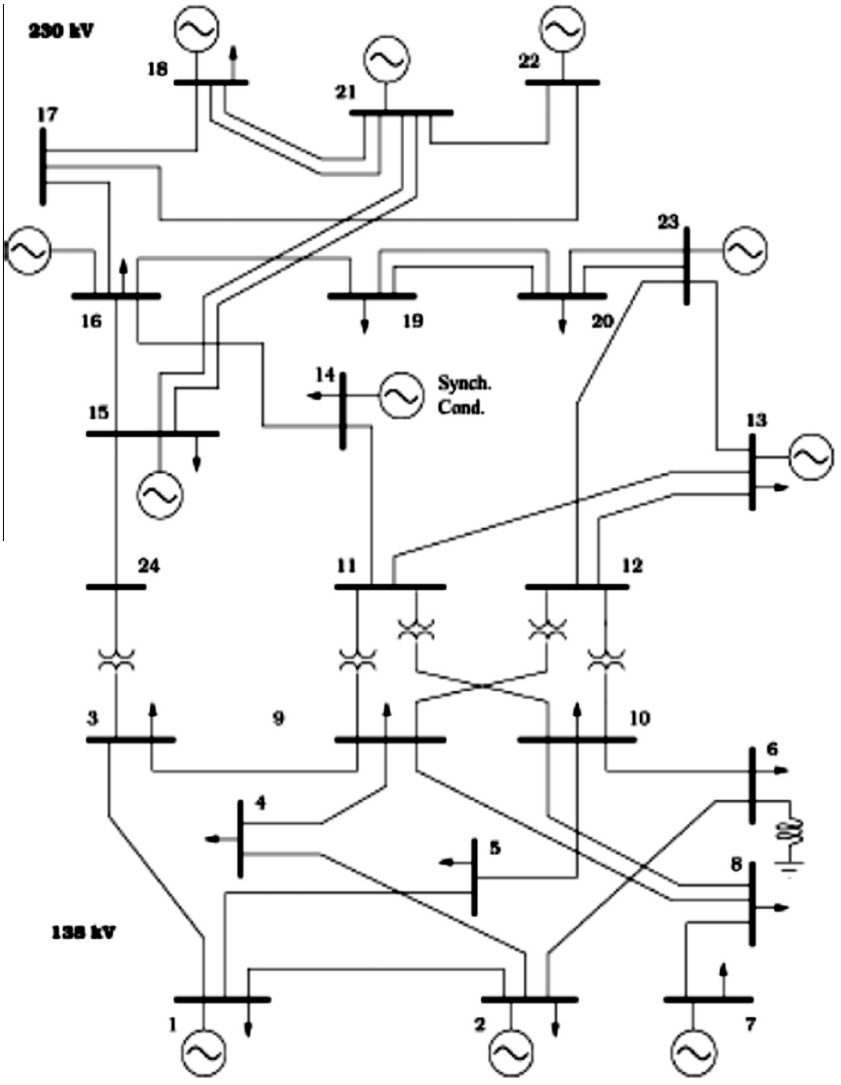

Fig. 3 Schematic of the IEEE RTS 24-bus system [68].

Table 1 Hourly load (MW) [68].

Hour	1	2	3	4	5	6
Load	1909	1795	1710	1681	1681	1710
Hour	7	8	9	10	11	12
Load	2109	2451	2707	2736	2736	2707
Hour	13	14	15	16	17	18
Load	2707	2707	2650	2679	2821	2850
Hour	19	20	21	22	23	24
Load	2850	2736	2593	2365	2080	1795

equations, parameters PS_s^{CRU}, PS_s^{CRD}, PS_s^{DRU}, and PS_s^{DRD} denote charge ramp-up, charge ramp-down, discharge ramp-up, and discharge tamp-down of the ESS, respectively.

$$PS_{s,t}^{Ch} \leqslant PS_{s,t-1}^{Ch} + PS_s^{CRU} BS_{s,t}^{Ch} \qquad \forall\, t \in T, \quad \forall\, s \in S \tag{50}$$

$$PS_{s,t}^{Ch} \geqslant PS_{s,t-1}^{Ch} - PS_s^{CRD} BS_{s,t}^{Ch} \qquad \forall\, t \in T, \quad \forall\, s \in S \tag{51}$$

$$PS_{s,t}^{Di} \leqslant PS_{s,t-1}^{Di} + PS_s^{DRU} BS_{s,t}^{Di} \qquad \forall\, t \in T, \quad \forall\, s \in S \tag{52}$$

$$PS_{s,t}^{Di} \geqslant PS_{s,t-1}^{Di} - PS_s^{DRD} BS_{s,t}^{Di} \qquad \forall\, t \in T, \quad \forall\, s \in S \tag{53}$$

Stored energy in the ESS can act as reserve power in case of contingencies. Therefore, this back-up power can assist the generation spinning reserve and be regarded as a second reserve in the system. Considering this issue, sum of the stored energy in the ESSs should be added to the generating units spinning reserve. In other words, reserve requirements of the system should be changed from (25)–(54) as follows:

$$P_t^{Res} = \sum_{s \in S} ES_{s,t} + \sum_{n \in N} PG_{n,t}^{Res} \qquad \forall\, t \in T \tag{54}$$

Complete proposed model

Finally, the proposed MILP model of the ESS integrated thermal unit commitment problem consists of the main unit commitment without ESS equations plus ESS modeling equations.

Table 2 Typical ESS characteristics [69].

ESS technology	Configuration	Total capital cost per power rating (€/kW)		Total capital cost per energy rating (€/kW h)		Round trip efficiency (%)		Lifetime (Year)	
		Min	Max	Min	Max	Min	Max	Min	Max
Pumped hydro	Conventional	1030	1675	96	181	0.70	0.82	50	60
Compressed air	Underground	774	914	48	106	0.70	0.89	20	40
	Aboveground	1286	1388	210	278	0.70	0.90	20	40
Battery	Lead-acid	1388	3254	346	721	0.70	0.90	5	15
	Li-ion	874	1786	973	1211	0.85	0.95	5	15

It should be noted that connecting links between thermal unit commitment model and ESS model are power balance and reserve requirements equations, modified from (15)–(40) and (25)–(54), respectively. In other words, final complete proposed model comprises the objective function (1), and Eq. (3)–(14), (16)–(17), (22)–(39), and (40)–(54).

Case study

The proposed formulation is implemented on the IEEE 24 bus reliability test system (RTS). The problem is implemented in GAMS [63] software and solved by CPLEX [64]. Schematic of the test system is presented in Fig. 3. Transmission lines data are as [68]. Synchronous condenser installed in bus 14 is detached because of using the DC power flow. The remained generating units are as [68] but with the following changes. In the original system all generating units are online initially. Here, we have a unit commitment problem and assume that only generating units 20–32 (units with low generation cost) are online initially. Also, shutdown cost of all units is equal to zero originally where are changed to the behalf of the start-up cost for each unit. The considered time span is 24 h and it is divided into 24 time periods. The non-linear cost function of the units is linearized with 10 equal segments and optimality gap of the CPLEX solver is set to 0.01 percent. The cost of the load shedding in each bus and at every time periods is fixed to 500 $/MW. Peak load of the system is equal to 2850 MW where hour-by-hour loading data for one year are provided before [68]. Day 352 of the year with most consumed energy is selected here as hourly load data, as presented in Table 1. For the sake of simplicity and without loss of generality, only one ESS type and one installation is considered in bus 10 of the system. Rated power of the ESS is equal to the 10 percent of the peak load, i.e. 285 MW. The ESS can store the rated power for 5 h, i.e. its rated energy is equal to 1425 MW h. Because of lacking relevant data, charge ramp-up, charge ramp-down, discharge ram-up, and discharge ramp-down are set to the rated power of the ESS. Typical ESS data for various technologies are provided [69] where information for bulk units is presented in Table 2. It is assumed that installed ESS is an underground compressed air system with 89 percent round-trip efficiency. Charge and discharge efficiencies both are set to the square of this value, i.e. 0.943.

The overall results of the base case simulation including start-up, shutdown, power generation, load shedding, and total operation cost for cases with and without ESS unit are given in Table 3. As the table shows, installing only one ESS unit in bus 10 of the system will reduce overall operation cost by 55,555 dollars per day. Amount of the cost reduction is equal to 6.8809 percent of the total cost which is a considerable value. As the results demonstrate, cost reduction is occurred in all cost components except load shedding. Also, governing cost component is power generation because of high share so its cost reduction percent is completely close to the total cost reduction. It is worth pointing out that besides cost coefficients, the shape of the load profile has a significant impact

Table 3 Base case operation cost results.

Cost component ($)	Without ESS	With ESS	Cost reduction	
			$	%
Start-up	1260	840	420	33.3333
Shutdown	1140	840	300	26.3158
Generation	804,985	750,150	54,835	6.8120
Load shedding	0	0	0	0
Total	807,385	751,829	55,555	6.8809

Table 4 ESS stored energy, charge, and discharge status.

Hour	Energy stored (MW h)	Power (MW)	
		Charge	Discharge
1	0.0	91.1	0.0
2	86.0	279.3	0.0
3	349.5	285.0	0.0
4	618.4	285.0	0.0
5	887.2	285.0	0.0
6	1156.1	285.0	0.0
7	1425.0	0.0	0.0
8	1425.0	0.0	77.0
9	1343.3	0.0	200.5
10	1130.8	0.0	96.0
11	1029.1	0.0	96.0
12	927.3	0.0	67.5
13	855.7	0.0	67.5
14	784.2	0.0	42.0
15	739.7	0.0	0.0
16	739.7	0.0	39.0
17	698.3	0.0	155.9
18	533.1	0.0	174.1
19	348.5	0.0	174.1
20	163.8	0.0	70.4
21	89.2	0.0	73.7
22	11.1	0.0	0.0
23	11.1	0.0	10.5
24	0	0.0	0.0

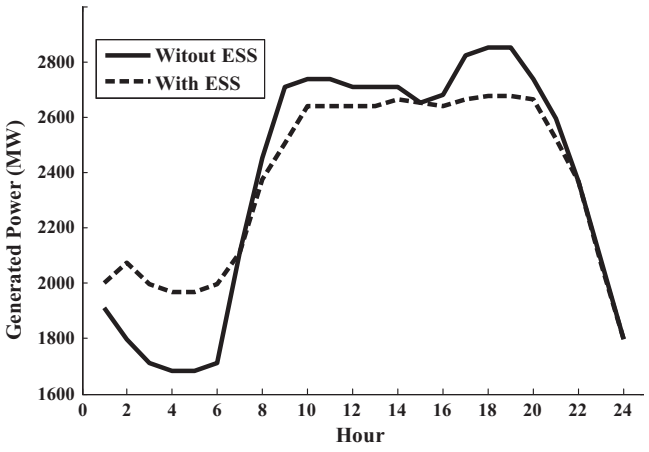

Fig. 4 Total generated power with and without ESS.

on the cost reduction percent because of the existence of the square term in the generation cost function. In other words, the most cost reduction will be yielded for a load profile with most variability. On the contrary, a constant load profile means no load leveling and no cost reduction as a result.

Total generated power of the units for both cases is depicted in Fig. 4. It should be noted that, in base case without ESS the total generated power is equal to the load demand. As the figure shows, optimal operation of the ESS results in proper load leveling by peak shaving and valley filling. More level load profiles will reach by increasing power and energy rating of the ESS.

Desired cost reduction may not be yielded unless the charge and discharge states and powers of the ESS be optimized through proper modeling. Optimal charge and discharge scheduling of the ESS along with hourly stored energy is provided in Table 4. As in the table, the ESS is charged during low demand periods and discharged during high demand periods. Obtained scheduling program helps system operators to decide on the optimum ESS state and power at every time period.

Besides base case results, sensitivity of the simulation results with respect to some dominant parameters of the ESS is analyzed. The parameters governing the results can be divided into ESS location and its technical characteristics. The results of changing the ESS installation bus are provided in Table 5. As the table confirms, average cost reduction percent is equal to 6.5590 where for most of the buses it is about 6.5–6.9. In addition, buses 7 and 21 are the worst and the best installation locations for the ESS in terms of cost reduction, respectively. Regarding obtained results, proposed formulation can be applicable to optimally site ESS among candidate locations in the system.

Three performance characteristics of the ESS that have a significant impact on the results are round-trip efficiency, power rating, and energy rating. Sensitivity of the cost reduction percent with respect to the power and energy ratings is given in Table 6. The percent of the operation cost reduction is quite sensitive to the energy and power ratings, as the results shows. It should be noted that after a certain value, further increase in power or energy rating does not influence the results and will be considered as overdesign. The application of this analysis could be in the power and energy sizing of the ESS.

Table 5 Sensitivity of the cost reduction with respect to the ESS installation bus.

Installation bus	Total operation cost with ESS ($)	Cost reduction	
		$	%
1	753,234	54,150	6.7069
2	752,519	54,865	6.7954
3	752,519	54,865	6.7954
4	755,006	52,378	6.4874
5	754,276	53,109	6.5779
6	764,169	43,216	5.3526
7	777,907	29,477	3.6510
8	753,761	53,623	6.6417
9	753,234	54,150	6.7069
10	751,829	55,555	6.8809
11	753,248	54,136	6.7051
12	753,248	54,136	6.7052
13	752,532	54,852	6.7938
14	752,170	55,215	6.8388
15	752,519	54,865	6.7954
16	753,363	54,022	6.6910
17	752,577	54,807	6.7883
18	752,409	54,975	6.8091
19	751,787	55,597	6.8861
20	753,262	54,122	6.7034
21	751,684	55,700	6.8989
22	752,532	54,852	6.7938
23	753,260	54,124	6.7037
24	753,234	54,150	6.7069
Minimum		3.6510 (Bus 7)	
Average		6.5590	
Maximum		6.8989 (Bus 21)	

Table 6 Sensitivity of the cost reduction percent with respect to the ESS power and energy ratings.

Rated energy (MW h)	Rated power as a percent of peak load (MW)				
	5.0	7.5	10	12.5	15.0
$1 \times P$	0.7296	1.5446	2.2086	2.0660	2.8035
$2 \times P$	2.2086	2.8035	3.4658	3.9171	4.4360
$3 \times P$	2.8570	3.3575	4.4646	5.3172	6.3155
$4 \times P$	3.3370	4.1852	5.7427	6.9005	7.9632
$5 \times P$	3.7779	5.1338	6.8809	8.3062	9.6739

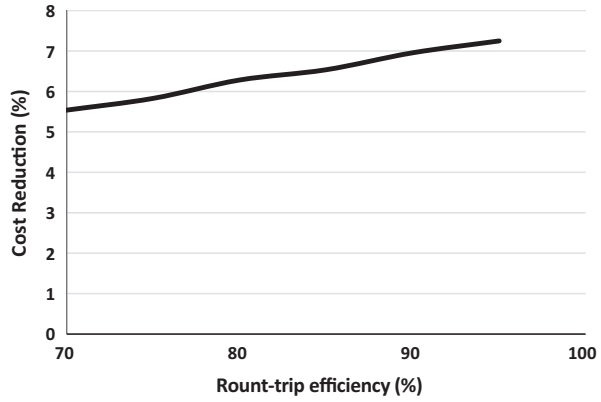

Fig. 5 Sensitivity of the cost reduction with respect to the ESS round-trip efficiency.

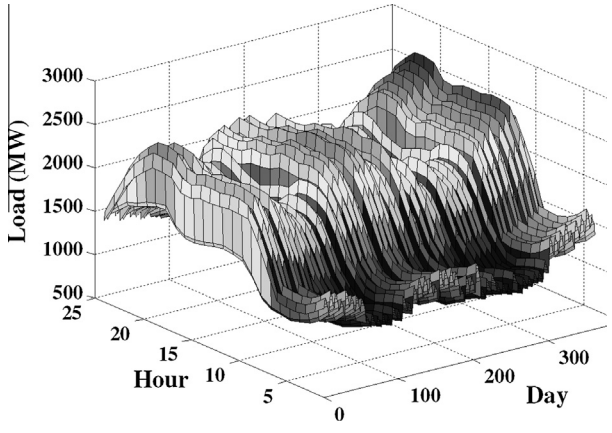

Fig. 6 IEEE RTS hour-by-hour yearly load [68].

The effect of the round-trip efficiency of the ESS on the results is considered in Fig. 5. In this analysis, charge and discharge efficiencies of the ESS are set equally with square of the values showed in the horizontal axis of the figure. As expected, the percent of the operation cost reduction is considerably sensitive to the charge/discharge efficiency. In other words, modest increase may increase cost reduction significantly.

At last but not least, it is essential to perform a cost/benefit analysis. As considered in the paper, the benefit is defined as operation cost reduction per day while for an ESS unit dominant cost factor is capital or investment cost. The capital cost in terms of energy and power rating for typical ESSs is provided in [69] and given in Table 2 for bulk units. Considering our assumption, i.e. using underground compressed air ESS, capital cost of the power rating varies from 774 to 914, where, this value for energy rating is from 48 to 106. Also, lifetime for this technology is between 20 and 40 years, as denoted by the table. Bear in mind that these values are gathered from the previous data not present data in addition to this fact that ESS technologies are progressing in terms of per unit cost reduction and lifetime improvement. As a result, we optimistically assume minimum power and energy capital cost and maximum lifetime for the installed ESS technology, that is, 774 €/kW, 48 €/kW h, and 40 years. It should be noted that capital cost is a one-shot value over ESS lifetime (in Euros as declared in [69]) while calculated operation cost reduction is a daily value (in Dollars). Regarding different time and currency scales of these values, they should be compared taking into account proper coefficients. Annuity factor (AF) can convert a capital cost to a yearly cost by considering interest rate (r) and lifetime (L) [70], as presented in (55):

$$\mathrm{AF} = \frac{r(1+r)^L}{(1+r)^L - 1} \tag{55}$$

In our case, we assume a 5% interest rate with 40 years lifetime as discussed above, resulting in 0.0582 annuity factor. Therefore, the converted yearly capital cost of the ESS will be yielded by multiplying annuity factor, power unit convert factor, and currency unit convert factor, as denoted by (56):

$$C^{Y}_{\mathrm{ESS}} = \mathrm{AF} \times \mathrm{FP}^{M}_{K} \times \mathrm{FC}^{E}_{D} \times \left(P^{\mathrm{Rated}}_{\mathrm{ESS}} \times \mathrm{CP}^{\mathrm{Rated}}_{\mathrm{ESS}} + E^{\mathrm{Rated}}_{\mathrm{ESS}} \times \mathrm{CE}^{\mathrm{Rated}}_{\mathrm{ESS}}\right) \tag{56}$$

In this equation, C^{Y}_{ESS}, AF, FP^{M}_{K}, FC^{E}_{D}, $P^{\mathrm{Rated}}_{\mathrm{ESS}}$, $\mathrm{CP}^{\mathrm{Rated}}_{\mathrm{ESS}}$, $E^{\mathrm{Rated}}_{\mathrm{ESS}}$, and $\mathrm{CE}^{\mathrm{Rated}}_{\mathrm{ESS}}$ denote ESS converted yearly capital cost, annuity factor (0.0582), power unit convert factor (1000), currency unit convert factor (1.07), installed power rating (28 MW), installed energy rating (1425 MW h), per unit cost of power rating (774 €/kW), and per unit cost of energy rating (774 €/kW h), respectively. With the abovementioned values, converted yearly capital cost of the installed ESS unit will be equal to 17,996,563 dollars. The hour-by-hour load of the considered IEEE RTS case study is presented in Fig. 6. As the figure shows, load profile shape is not changed considerably for various days of the year. We assume a constant load profile and consequently a constant operation cost reduction value for all days over horizon time (this assumption justifies load growth factor during 40 years lifetime of the ESS). Consequently, the expected cost reduction for one year will be equal to 20,277,575 dollars. Compared to the ESS yearly investment cost, installing the ESS unit will result in a 2,281,012 dollars net benefit per year. Although the expected obtained yearly benefit is an estimated value, it should be

noted that synergic utilization of the ESS applications discussed in the introduction, will justify computation errors so that obtained benefit will be completely competitive compared to the investment costs.

Conclusions

In the present paper, large-scale Energy Storage Systems (ESSs) have been modeled and integrated in the thermal unit commitment problem. The proposed model, Mixed Integer Linear Programming (MILP), ensures convergence to the global optimum while can be easily solved with well-known available solvers without problems of the practical large scale networks. The technical constraints of the thermal units operation and transmission network constraints have been considered in the model, too. The results of the simulations on the case study demonstrated that conducted load leveling through optimum storage management leads to considerable reduction in daily operation costs. In addition, optimal storage charge/discharge schedule of the ESS in order to achieve minimum cost operation has been obtained. Besides storage modeling and integration in UC, a comprehensive sensitivity analysis has been carried out with respect to installation size and technical characteristics of the ESS. Regarding generality of the proposed model, it can be utilized in various system studies including operation, planning, market clearing, and demand response.

Conflict of Interest

The authors have declared no conflict of interest.

Compliance with Ethics Requirements

This article does not contain any studies with human or animal subjects.

References

[1] Ibrahim H, Ilinca A, Perron J. Energy storage systems – characteristics and comparisons. Renew Sust Energ Rev 2008;12:1221–50.

[2] Vazquez S, Lukic SM, Galvan E, Franquelo LG, Carrasco JM. Energy storage systems for transport and grid applications. IEEE T Ind Electron 2010;57(12):3881–95.

[3] Mahlia TMI, Saktisahdan TJ, Jannifar A, Hasan MH, Matseelar HSC. A review of available methods and development on energy storage; technology update. Renew Sust Energ Rev 2014;33:532–45.

[4] Zhao H, Wu Q, Hu S, Xu H, Rasmussen CN. Review of energy storage system for wind power integration support. Appl Energ 2015;137:545–53.

[5] Hadjipaschalis I, Poullikkas A, Efthimiou V. Overview of current and future energy storage technologies for electric power applications. Renew Sust Energ Rev 2009;13(6):1513–22.

[6] Luo X, Wang J, Dooner M, Clarke J. Overview of current development in electrical energy storage technologies and the application potential in power system operation. Appl Energ 2015;137:511–36.

[7] Kyriakopoulos GL, Arabatzis G. Electrical energy storage systems in electricity generation: energy policies, innovative technologies, and regulatory regimes. Renew Sust Energ Rev 2016;56:1044–67.

[8] Wade NS, Taylor PC, Lang PD, Jones PR. Evaluating the benefits of an electrical energy storage system in a future smart grid. Energ Policy 2010;38(11):7180–8.

[9] Chatzivasileiadi A, Ampatzi E, Knight I. Characteristics of electrical energy storage technologies and their applications in buildings. Renew Sust Energ Rev 2013;25:814–30.

[10] Ribeiro PF, Johnson BK, Crow ML, Arsoy A, Liu Y. Energy storage systems for advanced power applications. Proc IEEE 2001;89(12):1744–56.

[11] Koohi-Kamali S, Tyagi VV, Rahim NA, Panwar NL, Mokhlis H. Emergence of energy storage technologies as the solution for reliable operation of smart power systems: a review. Renew Sust Energ Rev 2013;25:135–65.

[12] Kapsali M, Kaldellis JK. Combining hydro and variable wind power generation by means of pumped-storage under economically viable terms. Appl Energ 2010;87(11):3475–85.

[13] Barzin R, Chen JJ, Young BR, Farid MM. Peak load shifting with energy storage and price-based control system. Energy 2015;92:505–14.

[14] Li Z, Guo Q, Sun H, Wang J. Storage-like devices in load leveling: complementarity constraints and a new and exact relaxation method. Appl Energ 2015;151:13–22.

[15] Han X, Ji T, Zhao Z, Zhang H. Economic evaluation of batteries planning in energy storage power stations for load shifting. Renew Energ 2015;78:643–7.

[16] Zhuk A, Zeigarnik Y, Buzoverov E, Sheindlin A. Managing peak loads in energy grids: comparative economic analysis. Energ Policy 2016;88:39–44.

[17] Reihani E, Sepasi S, Roose LR, Matsuura M. Energy management at the distribution grid using a Battery Energy Storage System (BESS). Int J Elec Power 2016;77:337–44.

[18] Kloess M, Zach K. Bulk electricity storage technologies for load-leveling operation – an economic assessment for the Austrian and German power market. Int J Elec Power 2014;59:111–22.

[19] Sun Y, Wang S, Xiao F, Gao D. Peak load shifting control using different cold thermal energy storage facilities in commercial buildings: a review. Energ Convers Manage 2013;71:101–14.

[20] Islam M, Mekhilef S, Saidur R. Progress and recent trends of wind energy technology. Renew Sust Energ Rev 2013;21:456–68.

[21] Pandey AK, Tyagi VV, Jeyraj A, Selvaraj L, Rahim NA, Tyagi SK. Recent advances in solar photovoltaic systems for emerging trends and advanced applications. Renew Sust Energ Rev 2016;53:859–84.

[22] Suberu MY, Mustafa MW, Bashir N. Energy storage systems for renewable energy power sector integration and mitigation of intermittency. Renew Sust Energ Rev 2014;35:499–514.

[23] Diouf B, Pode R. Potential of lithium–ion batteries in renewable energy. Renew Energ 2015;76:375–80.

[24] Castillo A, Gayme DF. Grid-scale energy storage applications in renewable energy integration: a survey. Energ Convers Manage 2014;87:885–94.

[25] Rodrigues EMG, Godina R, Santos SF, Bizuayehu AW, Contreras J, Catalão JPS. Energy storage systems supporting increased penetration of renewables in islanded systems. Energy 2014;75:265–80.

[26] Bianchi M, Branchini L, De Pascale A, Melino F. Storage solutions for renewable production in household sector. Energ Proc 2014;61:242–5.

[27] Beaudin M, Zareipour H, Schellenberglabe A, Rosehart W. Energy storage for mitigating the variability of renewable electricity sources: an updated review. Energ Sust Develop 2010;14(4):302–14.

[28] Díaz-González F, Sumper A, Gomis-Bellmunt O, Villafáfila-Robles R. A review of energy storage technologies for wind power applications. Renew Sust Energ Rev 2012;16(4):2154–71.

[29] Kundur P, Paserba J, Ajjarapu V, Andersson G, Bose A, Canizares C, Hatziargyriou N, Hill D, Stankovic A, Taylor C,

Cutsem TV. Definition and classification of power system stability IEEE/CIGRE joint task force on stability terms and definitions. IEEE T Power Electr 2004;19(3):1387–401.
[30] Egido I, Sigrist L, Lobato E, Rouco L, Barrado A. An ultra-capacitor for frequency stability enhancement in small-isolated power systems: models, simulation and field tests. Appl Energ 2015;137:670–6.
[31] Kim JY, Jeon JH, Kim SK, Cho C, Park JH, Kim HM, Nam KY. Cooperative control strategy of energy storage system and microsources for stabilizing the microgrid during islanded operation. IEEE T Power Electr 2010;25(12):3037–48.
[32] Serban I, Teodorescu R, Marinescu C. Energy storage systems impact on the short-term frequency stability of distributed autonomous microgrids, an analysis using aggregate models. IET Renew Power Gener 2013;7(5):531–9.
[33] Han Y, Young PM, Jain A, Zimmerle D. Robust control for microgrid frequency deviation reduction with attached storage system. IEEE T Smart Grid 2015;6(2):557–65.
[34] Serban I, Marinescu C. Battery energy storage system for frequency support in microgrids and with enhanced control features for uninterruptible supply of local loads. Int J Elec Power 2014;54:432–41.
[35] Mercier P, Cherkaoui R, Oudalov A. Optimizing a battery energy storage system for frequency control application in an isolated power system. IEEE T Power Syst 2009;24(3):1469–77.
[36] Ngamroo I, Mitani Y, Tsuji K. Application of SMES coordinated with solid-state phase shifter to load frequency control. IEEE T Appl Supercon 1999;9(2):322–5.
[37] Seo HR, Kim GH, Park M, Yu IK, Otsuki Y, Tamura J, Kim SH, Sim K, Seong KC. Operating characteristic analysis of HTS SMES for frequency stabilization of dispersed power generation system. IEEE T Appl Supercon 2010;20(3):1334–8.
[38] Kim SY, Kim KM, Kim JG, Kim S, Park M, Yu IK, Lee S, Sohn MH, Kim HJ, Bae JH, Seong KC. Performance analysis of a toroid-type htssmes adopted for frequency stabilization. IEEE T Appl Supercon 2011;21(3):1367–70.
[39] Shirai Y, Nitta T, Shibata K. On-line monitoring of eigen-frequency and stability of power system by use of SMES. Int J Elec Power 2012;42(1):473–7.
[40] Egido I, Sigrist L, Lobato E, Rouco L, Barrado A. An ultra-capacitor for frequency stability enhancement in small-isolated power systems: models, simulation and field tests. Appl Energ 2015;137:670–6.
[41] Shah R, Mithulananthan N, Bansal RC. Damping performance analysis of battery energy storage system, ultracapacitor and shunt capacitor with large-scale photovoltaic plants. Appl Energ 2012;96:235–44.
[42] Döşoğlu MK, Arsoy AB. Transient modeling and analysis of a DFIG based wind farm with supercapacitor energy storage. Int J Elec Power 2016;78:414–21.
[43] Wang MH, Chen HC. Transient stability control of multimachine power systems using flywheel energy injection. IET Proc-Gener Transm Distrib 2005;152(5):589–96.
[44] Wang L, Yu JY, Chen YT. Dynamic stability improvement of an integrated offshore wind and marine-current farm using a flywheel energy-storage system. IET Proc-Renew Power Gener 2011;5(5):387–96.
[45] EPRI PEAC Corporation. EPRI-DOE handbook of energy storage for transmission & distribution applications. Washington (DC): Cosponsor by: US Department of Energy; 2003.
[46] Del Rosso AD, Eckroad SW. Energy storage for relief of transmission congestion. IEEE T Smart Grid 2014;5(2):1138–46.
[47] Khani H, DadashZadeh MR, Hajimiragha AH. Transmission congestion relief using privately owned large-scale energy storage systems in a competitive electricity market. IEEE T Power Syst 2015;PP(99):1.
[48] Vargas LS, Bustos-Turu G, Larrain F. Wind power curtailment and energy storage in transmission congestion management considering power plants ramp rates. IEEE T Power Syst 2015;30(5):2498–506.
[49] Eyer J, Iannucci J, Butler PC. Estimating electricity storage power rating and discharge duration for utility transmission and distribution deferral: a study for the DOE energy storage program. Sandia National Laboratories Technical report, 2005.
[50] Zhang F, Hu Z, Song Y. Mixed-integer linear model for transmission expansion planning with line losses and energy storage systems. IET Proc-Gener Transm Distrib 2013;7 (8):919–28.
[51] Konstantelos I, Strbac G. Valuation of flexible transmission investment options under uncertainty. IEEE T Power Syst 2015;30(2):1047–55.
[52] Saboori H, Abdi H. Application of a grid scale energy storage system to reduce distribution network losses. In: 18th electric power distribution conference; 2013. p. 1–5.
[53] Saboori H, Hemmati R, Jirdehi MA. Reliability improvement in radial electrical distribution networks by optimal planning of energy storage systems. Energy 2015;93(2):2299–312.
[54] Saboori H, Hemmati R, Abbasi V. Multistage distribution network expansion planning considering the emerging energy storage systems. Energ Convers Manage 2015;105:938–45.
[55] Wood AJ, Wollenberg BF. Power generation, operation, and control. John Wiley & Sons; 2012.
[56] Zhu J. Optimization of power system operation. John Wiley & Sons; 2015.
[57] Padhy NP. Unit commitment—a bibliographical survey. IEEE T Power Syst 2004;19:1196–205.
[58] Arroyo JM, Conejo J. Optimal response of a thermal unit to an electricity spot market. IEEE T Power Syst 2000;15:1098–104.
[59] Carrión M, Arroyo JM. A computationally efficient mixed-integer linear formulation for the thermal unit commitment problem. IEEE T Power Syst 2006;21:1371–8.
[60] Frangioni A, Gentile C, Lacalandra F. Tighter approximated MILP formulations for unit commitment problems. IEEE T Power Syst 2009;24:105–13.
[61] Morales-España G, Latorre JM, Ramos A. Tight and compact MILP formulation of start-up and shut-down ramping in unit commitment. IEEE T Power Syst 2013;28:1288–96.
[62] Ostrowski J, Anjos MF, Vannelli A. Tight mixed integer linear programming formulations for the unit commitment problem. IEEE T Power Syst 2012;27:39.
[63] Brooke A, Kendrick D, Meeraus A, Raman R, America U. The general algebraic modeling system. GAMS Development Corporation; 1998.
[64] Cplex I. 11.0 User's manual. Gentilly (France): ILOG SA; 2007, p. 32.
[65] Stott B, Jardim J, Alsaç O. DC power flow revisited. IEEE T Power Syst 2009;24(3):1290–300.
[66] Powell L. Power system load flow analysis. McGraw Hill Professional Series; 2004.
[67] Grünewald P, Cockerill T, Contestabile M, Pearson P. The role of large scale storage in a GB low carbon energy future: issues and policy challenges. Energ Policy 2011;39(9):4807–15.
[68] Wong P, Albrecht P, Allan R, Billinton R, Chen Q, Fong C, Haddad S, Li W, Mukerji R, Patton D, Schneider A, Shahidehpour M, Singh C. The IEEE reliability test system-1996. A report prepared by the reliability test system task force of the application of probability methods subcommittee. IEEE T Power Syst 1999;14(3):1010–20.
[69] Zakeri B, Syri S. Electrical energy storage systems: a comparative life cycle cost analysis. Renew Sust Energ Rev 2015;42:569–96.
[70] Park CS. Contemporary engineering economics. Prentice Hall; 2007.